

Optics Letters

Quantitative measurement of the orbital angular momentum of light with a single, stationary lens

SAMUEL N. ALPERIN,¹ ROBERT D. NIEDERRITER,² JULIET T. GOPINATH,^{2,3} AND MARK E. SIEMENS^{1,*}

¹Department of Physics and Astronomy, University of Denver, Denver, Colorado 80208, USA

²Department of Physics, University of Colorado, Boulder, Colorado 80309, USA

³Department of Electrical, Computer, and Energy Engineering, University of Colorado, Boulder, Colorado 80309, USA

*Corresponding author: msiemens@du.edu

Received 11 August 2016; revised 30 September 2016; accepted 4 October 2016; posted 4 October 2016 (Doc. ID 273263); published 26 October 2016

We show that the average orbital angular momentum (OAM) of twisted light can be measured simply and robustly with a single stationary cylindrical lens and a camera. Theoretical motivation is provided, along with self-consistent optical modeling and experimental results. In contrast to qualitative interference techniques for measuring OAM, we quantitatively measure non-integer average OAM in mode superpositions. © 2016 Optical Society of America

OCIS codes: (080.4865) Optical vortices; (140.3295) Laser beam characterization; (260.6042) Singular optics.

<http://dx.doi.org/10.1364/OL.41.005019>

Light can have two forms of angular momentum: *spin* angular momentum related to the polarization, and *orbital* angular momentum (OAM) arising from a helical phase front around a beam. As a result of these helical phase fronts and the resulting singularity at the center, light with OAM is often referred to as “twisted” or “vortex” light. While the spin angular momentum of light has been understood for nearly a century, in 1992 Allen *et al.* were the first to demonstrate that laser light can be made to carry well-defined OAM [1] and, since then, it has seen steadily increasing scientific and engineering interest. The interest in OAM has been driven largely by its promise in applications, including rotational control in optical tweezers [2] and super resolution stimulated emission depletion (STED) microscopy [3].

The measurement of OAM is a vibrant area of active research. The earliest OAM measurements used interference with a Gaussian reference beam, such that the number of dark fringes observed around a beam was equal to the absolute value of the OAM [4,5]. Other work showed that passing a beam with OAM through a cylindrical lens leads to an interference pattern at the lens focus; the dark fringes in this interference pattern yield an integer value of the OAM, and the direction of the skew gives the sign of OAM [6–9]. Recently, alternatives based on self-interference [10] or counting dark fringes due to diffraction from apertures of different shapes [11,12] or at the focus of a cylindrical lens [6] have been demonstrated. These methods only work for optical modes with clearly identifiable

patterns and, thus, have the disadvantage of being limited to nearest-integer assessment of OAM values. Such qualitative techniques cannot measure OAM mode mixtures or even assess the alignment quality for pure OAM mode generation, so quantitative measurement techniques capable of measuring non-integer OAM are needed.

An alternative method for measuring non-integer OAM is mode separation, which can be done in multiple ways, some of which include geometrical phase transformation from helical to linear using spatial light modulators [13] or custom phase optics [14], extended arrays of Dove prisms [15], or focusing the output of a forked diffraction grating into a single-mode fiber [16]. Other techniques, such as OAM density [17] and skew-angle measurements [18] could measure non-integer OAM, although this has not been explicitly demonstrated. These methods have various drawbacks, including high cost, custom fabrication, complicated setup, and slow speed.

In this Letter, we combine an analytical model with experimental results to show that average non-integer OAM can be measured quantitatively with only a single, stationary cylindrical lens and a CCD. Our measurement technique is motivated by the momentum space mapping of a lens; that is, a lens transforms incident photon momentum to position at the focal plane, as illustrated in Fig. 1. The small azimuthal momentum component in twisted light leads to an OAM-dependent skew at the focus of a cylindrical lens. We show that this skew can be connected quantitatively to the average OAM of the incident light and that these measurements are effective, even with highly multimode beams. This Letter moves beyond qualitative interference techniques for measuring OAM, the importance of which is demonstrated by the OAM measurements of vortex chain beams.

The angular momentum of a single photon relative to the center of a beam can be calculated from the classical mechanics definition of the angular momentum $\vec{L} = \vec{r} \times \vec{p}$ of a point particle, where (\vec{r}, \vec{p}) are the photon's in-plane distance from beam center and momentum, respectively. Defining the z -direction to be along the beam propagation, the angular momentum is

$$L_z = \vec{r} \times \vec{p} \cdot \hat{z} = xp_y - yp_x = \hbar(xk_y - yk_x), \quad (1)$$

where (x, y) are the Cartesian coordinates in the plane of the beam, and (p_x, p_y) are the in-plane photon momentum

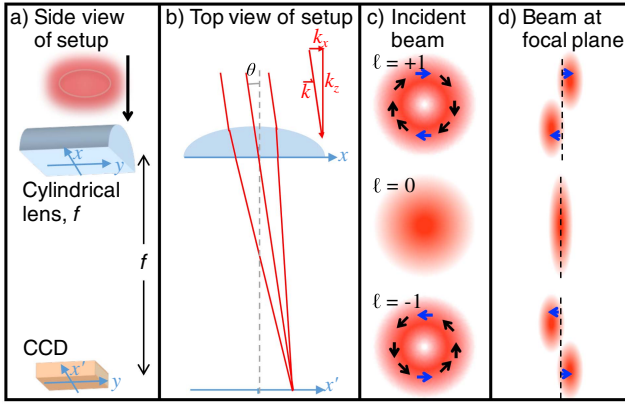


Fig. 1. Concept for simple OAM measurement with a cylindrical lens. (a) Side view of a beam incident on a cylindrical lens. (b) Top view illustrates how the direction at the lens is translated to the position at the focus. (c) Incident intensity profiles for different OAM values; the arrows show the transverse component of the Poynting vector. (d) CCD images at the focal plane for OAM values corresponding to the modes in (c). Blue arrows show how the OAM-induced angle of incidence on the cylindrical lens leads to a shift at the focus.

components. The right side of Eq. (1) follows from the fact that the linear momentum of light is related to the wavevector, \vec{k} , as $\vec{p} = \hbar\vec{k}$. The transverse components of the wavevector, k_x and k_y , give the local direction of propagation relative to the z -direction.

Now we want to relate the transverse wavevectors incident on the lens (k_x, k_y) to position in the focal plane of the cylindrical lens. For k_x , geometrical optics shows that $\tan(\theta) = x'/f = k_x/k_z$, where x' is the position in the focal plane along the same direction as x , f is the focal length of the lens, and θ is the transverse angle of incidence on the lens. Solving for k_x , repeating the calculation for k_y , and approximating $k_z \sim k = (2\pi/\lambda)$, we can write Eq. (1) as

$$L_z = \frac{2\pi\hbar}{f\lambda} (xy' - yx'), \quad (2)$$

where λ is the wavelength of the light. The $k_z \sim k$ approximation is a statement that the azimuthal momentum of twisted light is much smaller than $2\pi/\lambda$, which leads to a correction term on L_z of $\sim \lambda^2 \ell^2 / w^2 \hbar$, where ℓ is the OAM quantum number such that the single-photon OAM is $\ell\hbar$, and w is the beam radius. This correction is on the order of 10^{-6} for optical wavelengths and typical beam sizes and OAM. For a collection of photons, the average OAM can be written as [19]

$$\langle L_z \rangle = \frac{2\pi\hbar}{f\lambda} (\langle xy' \rangle - \langle yx' \rangle), \quad (3)$$

where $\langle \rangle$ indicates an average over an entire beam.

Our derivation arrives at the same results yielded by the treatment of the Poynting vector [20] or a raised operator method [21]. In addition, the expression for average OAM in Eq. (3) is closely related to the twist parameter used to characterize astigmatic beams [22,23], as has been noted by others [24]. Previous measurements of the twist parameter were made by careful beam profile measurements at numerous positions through the focus of both spherical and cylindrical lenses [23,25]. However, we note that each of the two terms in

parentheses in Eq. (3) can be directly measured at the focus of a cylindrical lens (since a cylindrical lens transforms a direction of incidence on the lens to position at the focal plane).

The mode at the focal plane of a cylindrical lens can be calculated analytically with a simple one-dimensional (1D) Fourier transform. This enables the calculation of the average OAM in the case of a known model.

To determine the OAM of a particular laser mode measured by a camera, we square the E-field to obtain intensity and then calculate $\langle yx' \rangle$, known as the x', y covariance $V_{x',y}$:

$$V_{x',y} = \langle yx' \rangle = \frac{\iint_{-\infty}^{\infty} |E(x',y)|^2 x' y dx' dy}{\iint_{-\infty}^{\infty} |E(x',y)|^2 dx' dy}. \quad (4)$$

The covariance calculation in the Fourier spatial domain provides a direct connection with the measured OAM per \hbar , ℓ_{meas} :

$$\ell_{\text{meas}} = \frac{2\pi\hbar}{f\lambda} (V_{x',y} - V_{y,x'})/\hbar. \quad (5)$$

In the case that there is reflectional symmetry (i.e., the intensity distribution on one side of a line matches the intensity on the other side if reflected about that line) about an axis $\pm \frac{\pi}{4}$ rad from the axis of the cylindrical lens, $V_{x,y'} = -V_{x',y}$ and, thus, Eq. (5) has only one covariance term:

$$\ell_{\text{meas}} = \frac{4\pi}{f\lambda} V_{x',y} = \frac{4\pi}{f\lambda} \frac{\iint_{-\infty}^{\infty} I(x',y) \ell x' y dx' dy}{\iint_{-\infty}^{\infty} I(x',y) \ell dx' dy}, \quad (6)$$

where $I(x',y)$ is the spatially resolved light intensity at the focal plane of the lens. This equation can be used to calculate the average OAM of a beam, given a CCD-recorded image of the beam at the focus of a cylindrical lens $I(x',y)$.

The general expression for a Laguerre–Gaussian (LG) mode with OAM ℓ and radial quantum number p can be written as [26]

$$E(r,\phi) = \sqrt{\frac{2p!}{\pi(p+|\ell|)!w}} \left(\frac{r\sqrt{2}}{w} \right)^{|\ell|} e^{-r^2/w^2} \times L_{p,|\ell|}[2r^2/w^2] e^{i\ell\phi}, \quad (7)$$

where $L_{p,|\ell|}[x]$ is a Laguerre polynomial, (r,ϕ) are the polar coordinate analogs to (x,y) , and w is the beam waist. Since we are only interested in the intensity at the focus, the Gouy phase is omitted. The 1D Fourier transform can be performed after mapping the LG mode in Eq. (7) to (x,y) . A Fourier transform for arbitrary integers (ℓ,p) is analytically intractable, but it can be performed for a particular integer values of (ℓ,p) .

To test the OAM measurement of a superposition of LG modes, we also modeled hypergeometric Gaussian (HyGG) modes, which can be represented as an infinite superposition of LG modes with fixed ℓ and varying p [27]. HyGG modes are important because they directly describe the twisted light generated by Gaussian illumination of a spiral phase plate or forked diffraction grating, rather than a single LG mode [28]. We calculate 1D Fourier transforms of HyGG beams to model the modes at the focal plane of a cylindrical lens, and show a few representative cases in the first row of Fig. 2. The measured OAMs from Eq. (6) for both LG and HyGG models match identically with expectations and with each other, even though HyGG beams are composed of many p modes, which reinforces that this measurement technique does not require pure LG modes as input.

In our experimental setup for demonstrating quantitative OAM measurement, shown in Fig. 3, light beams with

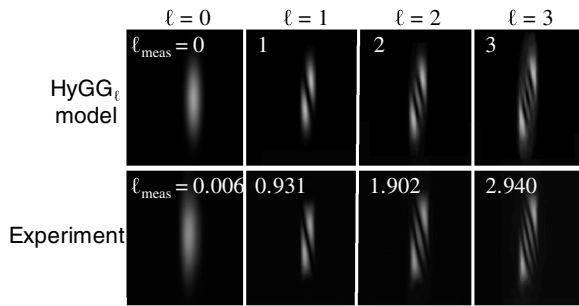


Fig. 2. Intensity modes at the focus of a cylindrical lens for an incident beam with OAM of $\ell = 0 \rightarrow 3$. The first row shows modeling results for a hypergeometric Gaussian HyGG (ℓ) mode, and the bottom row shows experimental results. Quantitative OAM values calculated from each image using Eq. (6) are indicated for each mode (ℓ_{meas}); the calculated values for the modeled images are calculated to be exact integers.

controllable OAM are generated by passing a collimated zeroth-order Gaussian beam ($w_0 = 2.6$ mm) from a HeNe laser ($\lambda = 633$ nm) through an amplitude modulated forked diffraction grating on a computer-controlled spatial light modulator. The OAM beam is then collimated with a two-lens telescope before passing through a cylindrical lens with a focal length of 1 m. A CCD is placed at the focus [Fig. 1(a)], and a series of images are acquired for input OAM values $\ell = -5 \rightarrow 5$.

This setup uses a spatial filter, an SLM, and a telescope to generate and collimate tunable light with OAM. The OAM measurement requires only a cylindrical lens and a CCD. The only calibration parameters are the lens to camera distance, the rotation angle of the cylindrical lens with respect to the CCD, and the collimation of the input beam. The following calibration method is a simple one-time procedure, and subsequent measurements can be made without further calibration. We start by passing a collimated beam through a cylindrical lens and placing the camera at the focus; collimation and lens-camera distance are not critical here because they will be optimized in the calibration. The calibration method is as follows. (1) Take OAM measurements at $\ell = \pm 5$ by acquiring images on the CCD and processing the intensity distribution using Eq. (6); rotate the cylindrical lens until the measurements are equal in magnitude and opposite in sign. (2) Fine-tune the collimation to optimize OAM measurement linearity with

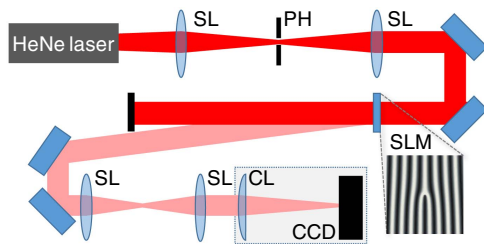


Fig. 3. Experimental setup for testing quantitative OAM measurement technique. SL, spherical lens; PH, pinhole; CL, cylindrical lens; SLM, spatial light modulator; CCD, CCD camera. Light diffracted from a forked grating on a SLM has tunable OAM (pink beam in the figure), which is quantitatively measured by the cylindrical lens and CCD. The OAM measurement portion of the setup is highlighted in the gray box with a dotted edge.

changing incident OAM. (3) Adjust the lens-camera distance to optimize the measurement slope ($\ell_{\text{meas}} - \ell$) to one.

As shown in Fig. 2, the images from a CCD camera at the focus of a cylindrical lens (bottom row) match the calculated 1D Fourier transforms of the corresponding HyGG modes (top row), which is expected for our OAM generation technique [27,28]. The measured images show integer OAM carrying beams, each with the corresponding integer number of dark fringes, in accordance with the model.

To quantify the OAM of a beam, each measured image at the focus of the cylindrical lens is treated as a two-dimensional intensity array $I(x', y)$, where $(x' = 0, y = 0)$ is the centroid of the intensity distribution, except in the case of non-integer OAM modes, for which $(x' = 0, y = 0)$ is defined by the intensity centroid of a reference Gaussian with the same center. The OAM is then calculated from Eq. (6). In the case of integer OAM beams, the resulting OAM measurements are expected to match the topological charges of the forked diffraction gratings used to make them. The measured OAM as a function of the expected integer OAM is shown in Fig. 4.

Although individual photons carry integer OAM, a superposition of photons can have a non-integer *average* OAM. Many sources of non-integer OAM, including direct mode addition with beam splitters or multimode mixing in fibers [23], produce beams with a single vortex and match the linear expectation shown in Fig. 4. In the special case of OAM beams produced from non-integer spiral phase plates or non-integer forked diffraction gratings [29], the superposition of topological charges leads to a phase singularity along a radial direction [10], as shown in the top row of Fig. 5. Individual OAM modes diffract at different angles off of this singularity, leading to the formation of a vortex chain perpendicular to the phase discontinuity [29]. This vortex chain introduces off-axis angular momentum, so the total OAM measured scales nonlinearly with the combined topological charge of the forked diffraction grating [10,29].

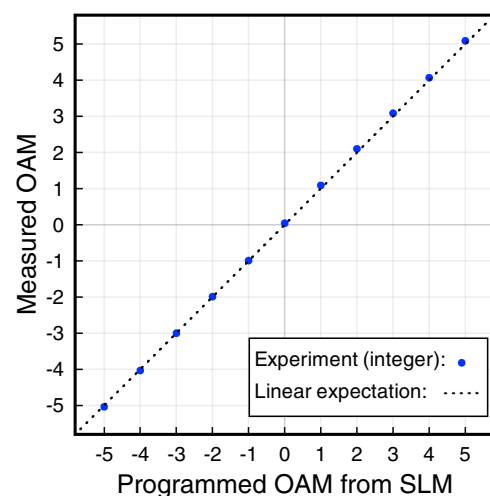


Fig. 4. Quantitative OAM measurements of integer OAM inputs from $\ell = -5 \rightarrow +5$. The dotted line corresponds to an ideal measurement of integer values, and all corresponding models for LG and HyGG modes fall on this line. Data are from experimental measurements using Eq. (6). The error bars showing the standard deviation of analyzing five sequential images are smaller than the dots.

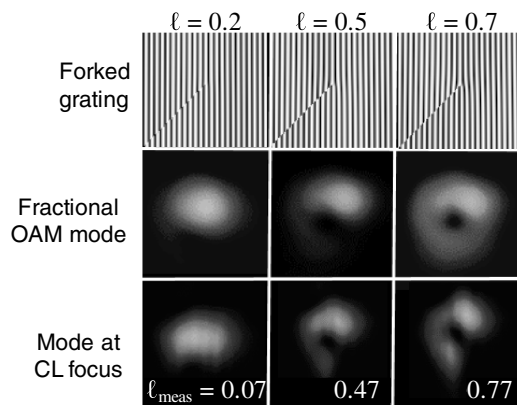


Fig. 5. Fractional OAM forked diffraction gratings (top row) with the corresponding fractional OAM modes (middle row). The bottom row shows modes at the focus of a cylindrical lens.

In order for a beam with a vortex chain to meet the symmetry requirement for a single-lens OAM measurement, the vortex chain must be oriented along a direction $\pm \frac{\pi}{4}$ from the axis of the lens [see the discussion before Eq. (6)]. We can do this by defining our forked diffraction gratings with a diagonal discontinuity (first row, Fig. 5) with respect to the axis of the cylindrical lens (vertical). Experimentally measured modes generated by these gratings and the resulting modes at the focus of a cylindrical lens are shown in the middle and bottom rows of Fig. 5, respectively.

Figure 6 shows the measured OAM of non-integer OAM beams as a function of the topological charge of the forked gratings that produced them. The nonlinearity of the non-integer OAM measurements is not an artifact of the OAM generation or measurement methods; in fact, our results are consistent with a theoretical prediction for non-integer OAM [29] (also shown in Fig. 6) which connects the nonlinearity of the average OAM to the formation of off-axis vortex chains. Our measurements are also in agreement with self-interference mode-fitting results from Leach *et al.* [10]. As seen in Fig. 5,

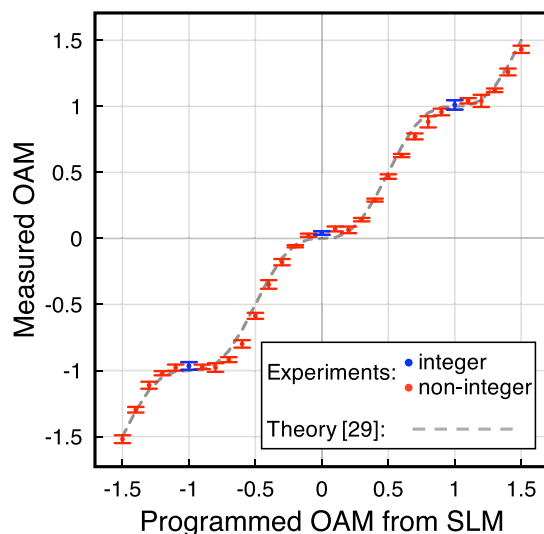


Fig. 6. Measurement from $\ell = -1.5 \rightarrow +1.5$ with steps of $\ell = 0.1$. The dotted line corresponds to the theoretical average OAM produced by a forked diffraction grating [29].

the OAM of beams with non-integer topological charge cannot be determined by visual mode examination.

In conclusion, we have proposed, modeled, and demonstrated a method for quantitative measurement of the average OAM of a beam of light. The method is simple, inexpensive, robust, and fast; it can accurately measure both integer and non-integer OAM of multimode beams. This measurement technique could find applications in many areas of OAM research for both scientific and technological applications.

Funding. National Science Foundation (NSF) (1509733, 1509928, 1553905, 1554704).

Acknowledgment. R. Niederriter received funding through the National Defense Science and Engineering Graduate Research Fellowship program.

REFERENCES

1. L. Allen, M. Beijersbergen, R. Spreeuw, and J. P. Woerdman, *Phys. Rev. A* **45**, 8185 (1992).
2. M. Padgett and R. Bowman, *Nat. Photonics* **5**, 343 (2011).
3. S. W. Hell and J. Wichmann, *Opt. Lett.* **19**, 780 (1994).
4. M. Soskin, V. Gorshkov, M. Vasnetsov, J. Malos, and N. Heckenberg, *Phys. Rev. A* **56**, 4064 (1997).
5. I. Basistiy, V. Y. Bazhenov, M. Soskin, and M. V. Vasnetsov, *Opt. Commun.* **103**, 422 (1993).
6. V. Denisenko, V. Shvedov, A. S. Desyatnikov, D. N. Neshev, W. Krolikowski, A. Volyar, M. Soskin, and Y. S. Kivshar, *Opt. Express* **17**, 23374 (2009).
7. A. Y. Bekshaev and A. Karamoch, *Opt. Commun.* **281**, 5687 (2008).
8. R. K. Singh, P. Senthilkumaran, and K. Singh, *Opt. Commun.* **270**, 128 (2007).
9. A. Y. Bekshaev, M. Soskin, and M. Vasnetsov, *Opt. Commun.* **241**, 237 (2004).
10. J. Leach, E. Yao, and M. J. Padgett, *New J. Phys.* **6**, 71 (2004).
11. L. E. De Araujo and M. E. Anderson, *Opt. Lett.* **36**, 787 (2011).
12. C.-S. Guo, L.-L. Lu, and H.-T. Wang, *Opt. Lett.* **34**, 3686 (2009).
13. G. C. G. Berkhout, M. P. J. Lavery, J. Courtial, M. W. Beijersbergen, and M. J. Padgett, *Phys. Rev. Lett.* **105**, 153601 (2010).
14. M. P. J. Lavery, D. J. Robertson, G. C. G. Berkhout, G. D. Love, M. J. Padgett, and J. Courtial, *Opt. Express* **20**, 2110 (2012).
15. J. Leach, M. J. Padgett, S. M. Barnett, S. Franke-Arnold, and J. Courtial, *Phys. Rev. Lett.* **88**, 257901 (2002).
16. A. Mair, A. Vaziri, G. Weihs, and A. Zeilinger, *Nature* **412**, 313 (2001).
17. A. Dudley, I. A. Litvin, and A. Forbes, *Appl. Opt.* **51**, 823 (2012).
18. J. Leach, S. Keen, M. J. Padgett, C. Saunter, and G. D. Love, *Opt. Express* **14**, 11919 (2006).
19. "Lasers and laser related equipment test methods for laser beam widths, divergence angles and beam propagation ratios. Part 1: stigmatic and simple astigmatic beams," ISO 11146-1:2005.
20. J. Serna and J. Movilla, *Opt. Lett.* **26**, 405 (2001).
21. J. Visser and G. Nienhuis, *Phys. Rev. A* **70**, 013809 (2004).
22. J. Serna, F. Encinas-Sanz, and G. Nemeş, *J. Opt. Soc. Am. A* **18**, 1726 (2001).
23. R. D. Niederriter, J. T. Gopinath, and M. E. Siemens, *Appl. Opt.* **52**, 1591 (2013).
24. B. Eppich, A. T. Friberg, C. Gao, and H. Weber, *Proc. SPIE* **2870**, 260 (1996).
25. A. Letsch and A. Giesen, *Proc. SPIE* **6101**, 610117 (2006).
26. A. E. Siegman, *Lasers* (University Science Books, 1986).
27. E. Karimi, G. Zito, B. Piccirillo, L. Marrucci, and E. Santamato, *Opt. Lett.* **32**, 3053 (2007).
28. A. Mawardi, S. Hild, A. Wiedera, and D. Meschede, *Opt. Express* **19**, 21205 (2011).
29. J. B. Götte, S. Franke-Arnold, R. Zambrini, and S. M. Barnett, *J. Mod. Opt.* **54**, 1723 (2007).